

Large Language Models as Topological Structure Enhancers for Text-Attributed Graphs

Shengyin Sun

City University of Hong Kong
shengysun4-c@my.cityu.edu.hk

Chen Ma[†]

City University of Hong Kong
chenma@cityu.edu.hk

Yuxiang Ren*

Advance Computing and Storage Lab
Huawei Technologies
renyuxiang1@huawei.com

Xuecang Zhang

Advance Computing and Storage Lab
Huawei Technologies
zhangxuecang@huawei.com

ABSTRACT

Inspired by the success of Large Language Models (LLMs) in natural language processing (NLP), recent works have begun investigating the potential of applying LLMs in graph learning. However, most of the existing work focuses on utilizing LLMs as node feature augmenters, leaving employing LLMs to enhance graph topological structures an understudied problem. In this paper, we are dedicated to leveraging the text comprehension and text generation capabilities of LLMs to refine and enhance the topological structure of text-attributed graphs (TAGs) under the node classification setting. First, we propose using LLMs to help remove unreliable edges and add reliable ones in the TAG. Specifically, we first let the LLM output the semantic similarity between node attributes through delicate prompt designs, and then perform edge deletion and edge addition based on the similarity. Second, we propose using pseudo-labels generated by the LLM to improve graph topology; we introduce pseudo-label propagation as a regularization to guide the graph neural network (GNN) in learning proper edge weights. Finally, we incorporate the two aforementioned graph topological refinements into the process of GNN training, and perform extensive experiments on four real-world datasets. The experimental results demonstrate the effectiveness of LLM-based graph topology refinement (achieving a 0.15%–2.47% performance gain on public benchmarks).

CCS CONCEPTS

• **Computing methodologies** → **Neural networks.**

KEYWORDS

Large Language Model; Graph Topological Refinement

* Equal contribution.

[†] Corresponding author: Chen Ma.

Permission to make digital or hard copies of all or part of this work for personal or classroom use is granted without fee provided that copies are not made or distributed for profit or commercial advantage and that copies bear this notice and the full citation on the first page. Copyrights for components of this work owned by others than ACM must be honored. Abstracting with credit is permitted. To copy otherwise, or republish, to post on servers or to redistribute to lists, requires prior specific permission and/or a fee. Request permissions from [permissions@acm.org](https://permissions.acm.org).

Conference acronym 'XX, June 03–05, 2018, Woodstock, NY

© 2018 Association for Computing Machinery.
ACM ISBN 978-1-4503-XXXX-X/18/06...\$15.00
<https://doi.org/XXXXXXXX.XXXXXXX>

ACM Reference Format:

Shengyin Sun, Yuxiang Ren, Chen Ma, and Xuecang Zhang. 2018. Large Language Models as Topological Structure Enhancers for Text-Attributed Graphs. In *Proceedings of Make sure to enter the correct conference title from your rights confirmation email (Conference acronym 'XX)*. ACM, New York, NY, USA, 10 pages. <https://doi.org/XXXXXXXX.XXXXXXX>

1 INTRODUCTION

Graphs, as a general data structure containing nodes and edges, are ubiquitous in various real-world scenarios such as molecular graphs in chemistry [13, 18] and social networks [24]. In the real world, the text-attributed graph (TAG) is also representative, which integrates both graph topological structure and text, enabling them to contain richer semantics. To effectively learn graph-structured data, graph neural networks (GNNs) have emerged. They introduce a message-passing mechanism to aggregate features from neighboring nodes, allowing the simultaneous incorporation of graph topology and node features [8, 28].

Note that GNNs only accept numerical features, whereas the attributes of nodes in TAGs are always in text format. Therefore, it is necessary to convert the textual attributes of nodes into embeddings that can be directly input into GNNs. In the classic GNN pipeline, the text attributes of nodes are usually encoded as shallow embeddings, such as by FastText [14] and Word2Vec [23]. However, recent studies argue that shallow embeddings have several limitations, such as the inability to effectively capture sentence-level semantics [22] and inadequacy in handling the phenomenon of polysemy [27]. To overcome them, recent works have introduced text encoding methods powered by language models (LMs). These LM-based methods obtain high-quality node representations (i.e., contextualized textual embeddings) by fine-tuning pre-trained LMs, such as BERT [6] and DeBERTa [9], on the specific task.

Although LMs have achieved satisfactory results in various tasks, researchers are still dedicated to further increasing the scale of model parameters to capture more complex linguistic patterns [15]. Recently, the vision of capturing complex linguistic patterns has been realized by large language models (LLMs). State-of-the-art LLMs such as ChatGPT [1] and GPT4 [25], with hundreds of billions of parameters, have demonstrated remarkable capabilities across a wide range of NLP tasks [3]. LLMs have achieved significant success in NLP tasks, but the application of their capabilities to

graph-structured data, such as TAGs, remains relatively underexplored. Early attempts focused on using LLMs to enhance node features and did not consider how to utilize LLMs for perturbing the graph structure. In this paper, we investigate how to harness LLMs to refine the topological structure of TAGs. The key motivation is that *we find TAGs contain many irrational/unreliable edges that can potentially have an adverse effect on the message-passing process in GNN* (we show in Fig. 1 that the proportion of potentially unreliable edges in the Cora and Citeseer datasets exceeds 15%), thus degrading the quality of learned node representations. Specifically, unlike other network architectures such as CNNs and MLPs that individually encode each entity (node), GNNs encode nodes through aggregation/propagation of node features. This means that if two nodes are connected by unreliable edges, their final aggregated representations will inevitably contain some noise (irrelevant features that do not reflect the properties of the nodes themselves). Therefore, it is necessary to remove unreliable edges through graph topology refinement.

To mitigate the impact of unreliable edges on model performance, we resort to LLMs for assistance. First, we explore the potential of LLMs in performing edge deletion and addition on TAGs. Specifically, through careful prompt design, we let the LLM output the relatedness (i.e., the semantic-level similarity) between two nodes in the TAG based on their textual attributes. Based on the obtained semantic-level similarity, we perform edge deletion and addition on the original graph, where we manage to keep (or add) edges between nodes with higher similarity and delete (or not add) edges between nodes with lower similarity. Second, we investigate leveraging pseudo-labels generated by LLMs to improve the graph topology, where we propose to incorporate pseudo-labels generated by LLMs into GNN training. In particular, we introduce the propagation of pseudo-labels as a regularization to guide the model in learning proper edge weights that benefit the separation of different node classes (i.e., enabling nodes with a high probability of belonging to the same class to connect more strongly, while promoting a better separation of nodes with a high probability of belonging to different classes). Finally, we combine the two proposed graph topology refinement methods with the LM-based GNN training. The contributions of this paper are as follows:

- Integrating LLMs with graph-structured data is a challenging problem, and most of the existing works only focus on using LLMs for node feature enhancement. In this paper, we make the first attempt at employing LLMs to improve graph topological structure.
- Two LLM-based graph topology refinement approaches are proposed. One involves using carefully crafted prompt statements to make the LLM generate semantic-level similarity between nodes. The generated similarity can be used to guide the addition of reliable edges and the removal of unreliable ones. The other involves using high-quality pseudo-labels generated by the LLM for pseudo-label propagation. The process of pseudo-label propagation is introduced as a regularization for the GNN training, leading the model to learn proper edge weights, thereby achieving the goal of improving graph topology.
- We combine the above two LLM-based graph topology refinement methods with conventional GNN training and provide theoretical

analysis to justify the benefits brought by the LLM-based graph topology refinement. The experimental results demonstrate the superiority of the proposed methods.

2 PRELIMINARY

2.1 Notations

Sets are denoted by calligraphic letters (e.g., \mathcal{S}). $|\cdot|$ denotes the number of elements in the set (e.g., $|\mathcal{S}|$). Matrices and vectors are denoted as bold upper case letters (e.g., \mathbf{X}) and bold lower case letters (e.g., \mathbf{x}), respectively. Superscript $(\cdot)^T$ denotes transpose for matrices or vectors. $\mathbb{R}^{m \times n}$ represents a real matrix space of dimension $m \times n$. $\mathbf{H}[i, :]$ is the i -th row of \mathbf{H} . $\mathbf{H}(i, j)$ represents the (i, j) -th element in the matrix \mathbf{H} . $\|\mathbf{v}\|$ is the norm of \mathbf{v} .

2.2 Text-attributed Graph

Define the TAG as $\mathcal{G} = \{\mathcal{V}, \mathcal{E}, \mathcal{X}, \mathbf{A}\}$, where \mathcal{V} is the set of nodes, \mathcal{E} is the set of edges, \mathcal{X} is a set of text attributes, and $\mathbf{A} \in \mathbb{R}^{|\mathcal{V}| \times |\mathcal{V}|}$ represents an adjacency matrix. More specifically, for each node v_i in \mathcal{V} , it corresponds to a piece of text $x_i \in \mathcal{X}$. If there is an edge between v_i and v_j , then $\mathbf{A}_{ij} = 1$; otherwise, $\mathbf{A}_{ij} = 0$. Under the node classification setting, v_i also corresponds to a label y_i that indicates which category the text attribute of node v_i belongs to.

2.3 Graph Neural Network

Mathematically, the representation of node u at the l -th GNN layer \mathbf{h}_u^l can be expressed as:

$$\mathbf{h}_u^l = f^l(\Phi; \mathcal{X}, \mathbf{A}) = \text{UPDATE} \left(\mathbf{h}_u^{l-1}, \text{AGG} \left(\left\{ \mathbf{h}_v^{l-1}, v \in \mathcal{N}_u \right\} \right) \right), \quad (1)$$

where \mathcal{N}_u is the set of neighbors of node u , AGG is the operation of aggregating messages, UPDATE is the operation of updating node u 's representation by using its previous representation and aggregated messages. For the sake of simplicity, the AGG and UPDATE operation in the l -th layer can be further abstracted into a parameterized function $f^l(\cdot)$ with the learnable parameters Φ .

3 METHODOLOGY

3.1 Necessity of Graph Topology Enhancement

• **The topology enhancement is neglected by existing LLM-GNN works.** A straightforward approach to combining LLMs and GNNs is to utilize the text generation capability of LLMs to enrich the input of GNNs. Employing LLMs as attribute enhancers is exemplified in works such as: (i) TAPE [10]—LLM is used to generate pseudo-labels for each node and is required to provide explanations for generating such pseudo-labels. These pseudo-labels and explanations are concatenated with the original text attributes as input for the GNN; (ii) KEA [4]—LLM is employed to extract technical terms from the original text attributes and is tasked with elaborating on these terms in detail. The generated technical terms with descriptions, along with the original text attributes, are then encoded by the GNN. However, these works overlook a crucial point that distinguishes the GNN from other architectures (such as the CNN): GNNs encode nodes through the aggregation/propagation of node features, rather than encoding nodes individually. *In other words, it is challenging to ensure the quality of the final representation (after aggregation) of a node when it is connected to noisy nodes*

through unreliable edges, no matter how its own features are enhanced. Therefore, we argue that the LLM-based topology enhancement is as important as the LLM-based attribute enhancement.

• **Observations from public datasets.** We investigate the proportion of potentially unreliable edges¹ in public datasets, as shown in Fig 1. Overall, the proportion of potential unreliable edges cannot be ignored (averaging over 15%). Taking Citeseer as an example, among edges where at least one endpoint belongs to the class “0”, the proportion of potentially unreliable edges exceeds 60%. This suggests that nodes of class “0” exhibit a high probability of connecting to unrelated nodes, which, in turn, can lead to blurred boundaries between the representations of nodes with class “0” and those of nodes with other classes after feature aggregation. To further demonstrate the potential of topology enhancement, we explore the impact of removing these potentially unreliable edges. As shown in Fig. 2, the accuracy steadily improves with the increasing delete ratio, which aligns with our previous analysis.

3.2 LLM-based Edge Deletion and Addition

LLMs have introduced a novel paradigm called “*pre-train, prompt, and predict*”. Under this paradigm, the LLM first undergoes pre-training in large-scale text datasets to learn general knowledge. Then, instead of fine-tuning the pre-trained model for each downstream task, the pre-trained model is prompted with a human-readable prompt according to the specific downstream task. The model generates the output based on the prompt and given input, without any task-specific fine-tuning of the model parameters.

From the perspective of the LLM’s input/output, the edge deletion and the edge addition share the same form of prompt paradigm. Specifically, we need to input the texts of the two endpoints (corresponding to a certain edge) into the LLM and guide the LLM to

¹A potentially unreliable edge refers to an edge connecting two endpoints belonging to distinct classes.

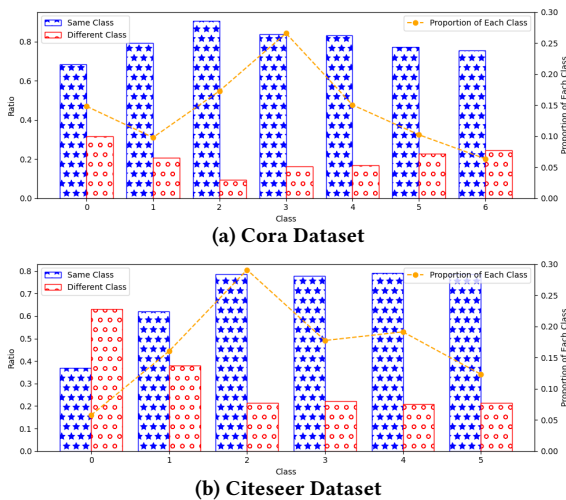


Figure 1: The proportion of edge endpoints with the same/different classes.

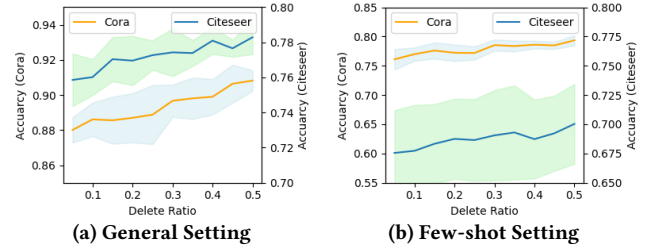


Figure 2: The impact of removing potentially unreliable edges on classification accuracy.

output its judgment on deleting or adding the edge, i.e.,

$$r_{ij} = \text{LLM}(\text{Prompt}(x_i, x_j)), \quad x_i, x_j \in \mathcal{X}, \quad (2)$$

where x_i and x_j are text attributes corresponding to the endpoints, $\text{Prompt}(\cdot)$ is the designed prompt format, and r_{ij} is the response text generated by the LLM. The well-designed prompt structure $\text{Prompt}(\cdot)$ for the edge deletion/addition is as follows:

Your task is to calculate the similarity between the given two papers. Here are some examples, where the input is the information for paper A and paper B, and the output is the estimated related ratio between paper A and paper B:

Example 1:

[Input] Paper A: Title: [paper title ...] Abstract: [paper abstract ...] Paper B: Title: [paper title ...] Abstract: [paper abstract ...]

[Output] Estimated Related Ratio between Paper A and Paper B: 0.x

Example 2:

[Input]... [Output]...

Example 3:

[Input]... [Output]...

...

Please return the similarity between the following two papers and briefly explain the reason:

Paper A:

Title: [paper title ...] Abstract: [paper abstract ...]

Paper B:

Title: [paper title ...] Abstract: [paper abstract ...]

Your return form is: Related ratio = ***, Reason: ***.

In the aforementioned prompt structure, we first describe the task to the LLM, that is, to estimate the similarity between two papers based on their titles and abstracts. To help the LLM better understand the task and prevent it from generating meaningless numbers, we then provide multiple examples as references. Finally, we include the text attributes related to the two endpoints (i.e., paper A and paper B), and request the LLM to output its estimations.

After obtaining the similarity estimations given by the LLM, we can use a threshold-based method to determine which edges need to be added or removed, i.e.,

$$A_{A-D}(i, j) = \begin{cases} 1, & \text{if } \text{Extract}(r_{ij}) > \xi \\ 0, & \text{if } \text{Extract}(r_{ij}) \leq \xi \end{cases} \quad (3)$$

where A_{A-D} is the adjacency matrix of the final refined graph, $\text{Extract}(\cdot)$ is a function that extracts similarity numbers from LLM’s response text, ξ is a preset threshold.

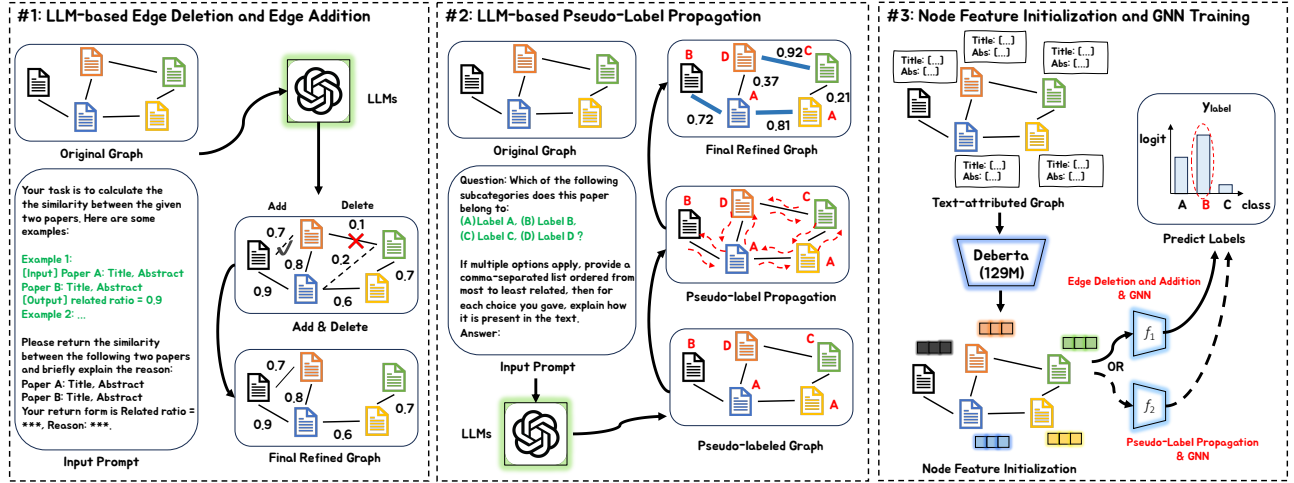


Figure 3: The overview of the proposed method. In the LLM-based edge deletion and edge addition (#1), LLM is used to filter unreliable edges and add reliable edges. In the LLM-based pseudo-label propagation (#2), LLM is used as a pseudo-label generator to guide the model in learning appropriate edge weights. The above two methods are essentially optimizing the graph topology. Therefore, they can be easily integrated into GNN training (#3) to boost model performance on downstream tasks.

3.3 LLM-based Pseudo-label Propagation

In this section, we first prompt the LLM to give pseudo-labels based on the text attributes of nodes. For convenience, we take the Citeseer dataset as an example to describe. The prompt structure on the Citeseer dataset is as follows:

The title and abstract of the paper are as follows: Title: [paper title ...] Abstract: [paper abstract ...]

Question: Which of the following subcategories does this paper belong to: (A) Agents, (B) Artificial Intelligence, (C) Database, (D) Human Computer Interaction, (E) Machine Learning, (F) Information Retrieval? If multiple options apply, provide a comma-separated list ordered from most to least related, then for each choice you gave, explain how it is present in the text.

Answer:

After obtaining the response text from the LLM, we choose the category that the LLM thinks the node v_i is most likely to belong to (the category ranked first in the response text) as the pseudo-label y_i^p . Inspired by the work [34], we hope to utilize the pseudo-labels generated by the LLM to optimize edge weights (in a label propagation manner) so that important edges can be highlighted in the message passing of GNNs. Formally, the LLM-based pseudo-label propagation containing K iterations can be written as:

$$\begin{cases} \mathbf{Y}^{(0)} = [\mathbf{y}_1^{(0)}, \dots, \mathbf{y}_{|\mathcal{V}|}^{(0)}]^\top, \\ \mathbf{Y}^{(k)} = \bar{\mathbf{A}}\mathbf{Y}^{(k-1)} = [\mathbf{y}_1^{(k)}, \dots, \mathbf{y}_{|\mathcal{V}|}^{(k)}]^\top, k = 1, \dots, K, \end{cases} \quad (4)$$

where $\mathbf{Y}^{(0)}$ is the initial label matrix for the label propagation, $\mathbf{y}_i^{(0)}$ for $i = 1, \dots, |\mathcal{V}|$ is the one-hot label indicator vector generated according to the y_i^p , $\bar{\mathbf{A}} = \mathbf{D}^{-\frac{1}{2}}\mathbf{A}\mathbf{D}^{-\frac{1}{2}}$ is the normalized adjacency matrix (consistent with the normalization method in the GCN [17]) with the learnable adjacency matrix \mathbf{A} and the diagonal degree

matrix \mathbf{D} for \mathbf{A} . The optimal edge weights can be obtained by minimizing the loss of predicted labels by the LLM-based pseudo-label propagation, i.e.,

$$\mathbf{A}^* = \arg \min_{\mathbf{A}} \frac{1}{|\mathcal{V}_{\text{train}}|} \sum_{v_i \in \mathcal{V}_{\text{train}}} \mathcal{L}_{\text{CE}}(\mathbf{y}_i^{\text{llm-lpa}}, \mathbf{y}_i), \quad (5)$$

where \mathbf{A}^* is the optimized graph topology, \mathcal{L}_{CE} is the cross-entropy loss, $\mathcal{V}_{\text{train}}$ is the training set containing labeled nodes, $\mathbf{y}_i^{\text{llm-lpa}}$ is the predicted label distribution of node v_i after K iterations of propagation (i.e., $\mathbf{y}_i^{\text{llm-lpa}} = \mathbf{y}_i^{(K)}$), and \mathbf{y}_i is the true one-hot label of node v_i . It should be noted that Eq. (5) merely demonstrates how to utilize the pseudo-labels from LLMs to help optimize the graph topology. In the next section, we will elaborate in more detail on how to integrate the LLM-based pseudo-label propagation into GNN training and train the whole model in an end-to-end manner.

3.4 Feature Initialization and GNN Training

In order to perform node feature initialization, we employ the pre-trained LM DeBERTa-base [9] to encode the text attribute x_i of the node v_i into the vectorial feature, i.e.,

$$\mathbf{h}_i = \text{LM}(x_i), v_i \in \mathcal{V}, x_i \in \mathcal{X}, \quad (6)$$

where \mathbf{h}_i is the text embedding for the node v_i , $\text{LM}(\cdot)$ represents the LM model DeBERTa-base. To extract the most informative textual features tailored for the downstream task, we follow the previous research by fine-tuning the LM [10]. More specifically, we apply a multi-layer perceptron (MLP) to the output of the LM and minimize the cross-entropy loss between the LM's predictions and the ground truth labels for each node.

For the method of LLM-based edge deletion and edge addition, we can perform the GNN training by directly utilizing the adjacency matrix $\mathbf{A}_{\text{A-D}}$ (see Section 3.2 for details). Formally, the process of

message passing and model optimization can be written as follows:

$$\begin{cases} \mathbf{H}^{(k)} = \sigma(\bar{\mathbf{A}}_{\text{A-D}} \mathbf{H}^{(k-1)} \mathbf{W}^{(k-1)}), k = 1, \dots, K, \\ \mathbf{W}^* = \arg \min_{\mathbf{W}} \frac{1}{|\mathcal{V}_{\text{train}}|} \sum_{v_i \in \mathcal{V}_{\text{train}}} \mathcal{L}_{\text{CE}}(y_i^{\text{gcn}}, y_i), \end{cases} \quad (7)$$

where $\sigma(\cdot)$ is an activation function, $\mathbf{W}^{(k)}$ is a learnable weight matrix in the k -th layer, $\bar{\mathbf{A}}_{\text{A-D}}$ is the normalized adjacency matrix for $\mathbf{A}_{\text{A-D}}$, $\mathbf{H}^{(k)}$ is the output matrix of the k -th layer (the initialization of \mathbf{H} is based on the Eq. (6), i.e., $\mathbf{H}^{(0)} = [\mathbf{h}_1, \dots, \mathbf{h}_{|\mathcal{V}|}]^\top$), \hat{y}_i^{gcn} represents the predicted label distribution of node v_i by using GCN in Eq. (7), \mathbf{W} denotes learnable parameters in the whole model, and \mathbf{W}^* is the optimized parameters.

For the LLM-based pseudo-label propagation, the process of model optimization and topology optimization can be written as:

$$\begin{aligned} \mathbf{W}^*, \mathbf{A}^* = \arg \min_{\mathbf{W}, \mathbf{A}} \frac{1}{|\mathcal{V}_{\text{train}}|} \sum_{v_i \in \mathcal{V}_{\text{train}}} & \left[\mathcal{L}_{\text{CE}}(y_i^{\text{gcn}}, y_i) \right. \\ & \left. + \lambda \mathcal{L}_{\text{CE}}(y_i^{\text{lpa}}, y_i) + \beta \mathcal{L}_{\text{CE}}(y_i^{\text{llm-lpa}}, y_i) \right], \end{aligned} \quad (8)$$

where λ and β are hyper-parameters, y_i^{lpa} and $y_i^{\text{llm-lpa}}$ are two label distributions obtained from two different label propagation methods. Specifically, $y_i^{\text{llm-lpa}}$ is the label distribution obtained from the initial label matrix constructed using the pseudo-labels generated by the LLM (see Eq. (4) for details), while y_i^{lpa} is the label distribution obtained from the initial label matrix constructed using the true labels from the training set (with the one-hot encoded labels for nodes outside the training set initialized as default values) [34].

3.5 Theoretical Justification

The overall framework is provided in Fig. 3. Essentially, the LLM-based graph topology refinement approaches proposed in the above sections aim to refine the message-passing process by applying hard/soft masks to graphs. In this section, we harness the shrinking theory [19, 34, 35] to understand the benefits of refining the message passing process. Define the measure of embedding variation [38] on graphs as:

$$\mathcal{M}(\mathbf{H}^{(k)}) = \frac{1}{2} \sum_{i=1}^{|\mathcal{V}|} \sum_{j=1}^{|\mathcal{V}|} \left\| \frac{\mathbf{A}(i, j)}{\mathbf{D}(i, i)} \mathbf{h}_i^{(k)} - \frac{\mathbf{A}(j, i)}{\mathbf{D}(j, j)} \mathbf{h}_j^{(k)} \right\|^2, \quad (9)$$

where $\mathbf{A}, \mathbf{D}, \mathbf{H}^{(k)}$ are the previously defined adjacency matrix, diagonal degree matrix, and embedding matrix, respectively. For the convenience of the following derivation, we rewrite $\mathcal{M}(\mathbf{H}^{(k)})$ as $\sum_{i=1}^{|\mathcal{V}|} \mathcal{M}_i(\mathbf{h}_i^{(k)})$. Utilizing the vector form of Taylor's theorem, we

have

$$\begin{aligned} \sum_{i=1}^{|\mathcal{V}|} \mathcal{M}_i(\mathbf{h}_i^{(k)} - \eta \nabla \mathcal{M}_i(\mathbf{h}_i^{(k)})) &= \sum_{i=1}^{|\mathcal{V}|} \left\{ \mathcal{M}_i(\mathbf{h}_i^{(k)}) - \right. \\ & \left. \left[\eta \nabla \mathcal{M}_i(\mathbf{h}_i^{(k)}) \right]^\top \int_0^1 \nabla \mathcal{M}_i(\mathbf{h}_i^{(k)} - \theta \eta \nabla \mathcal{M}_i(\mathbf{h}_i^{(k)})) d\theta \right\} \\ &= \sum_{i=1}^{|\mathcal{V}|} \left\{ \mathcal{M}_i(\mathbf{h}_i^{(k)}) - \left[\eta \nabla \mathcal{M}_i(\mathbf{h}_i^{(k)}) \right]^\top \nabla \mathcal{M}_i(\mathbf{h}_i^{(k)}) - \left[\eta \nabla \mathcal{M}_i(\mathbf{h}_i^{(k)}) \right]^\top \right. \\ & \times \int_0^1 \left[\nabla \mathcal{M}_i(\mathbf{h}_i^{(k)} - \theta \eta \nabla \mathcal{M}_i(\mathbf{h}_i^{(k)})) - \nabla \mathcal{M}_i(\mathbf{h}_i^{(k)}) \right] d\theta \left. \right\} \\ &\leq \sum_{i=1}^{|\mathcal{V}|} \left\{ \mathcal{M}_i(\mathbf{h}_i^{(k)}) - \left[\eta \nabla \mathcal{M}_i(\mathbf{h}_i^{(k)}) \right]^\top \nabla \mathcal{M}_i(\mathbf{h}_i^{(k)}) + \right. \\ & \left. \int_0^1 \left\| \eta \nabla \mathcal{M}_i(\mathbf{h}_i^{(k)}) \right\| \left\| \nabla \mathcal{M}_i(\mathbf{h}_i^{(k)} - \theta \eta \nabla \mathcal{M}_i(\mathbf{h}_i^{(k)})) - \nabla \mathcal{M}_i(\mathbf{h}_i^{(k)}) \right\| d\theta \right\}. \end{aligned} \quad (10)$$

Note that

$$\begin{aligned} \mathbf{h}_i^{(k)} - \frac{1}{2} \nabla \mathcal{M}_i(\mathbf{h}_i^{(k)}) &= \mathbf{h}_i^{(k)} - \sum_{j=1}^N \left[\frac{\mathbf{A}(i, j)}{\mathbf{D}(i, i)} \mathbf{h}_i^{(k)} - \frac{\mathbf{A}(i, j)}{\mathbf{D}(j, j)} \mathbf{h}_j^{(k)} \right] \\ &= \mathbf{h}_i^{(k+1)}, \end{aligned} \quad (11)$$

the Eq. (10) can be further expressed as:

$$\begin{aligned} \sum_{i=1}^{|\mathcal{V}|} \mathcal{M}_i(\mathbf{h}_i^{(k)} - \eta \nabla \mathcal{M}_i(\mathbf{h}_i^{(k)})) &\leq \sum_{i=1}^{|\mathcal{V}|} \left\{ \mathcal{M}_i(\mathbf{h}_i^{(k)}) - \left[\eta \nabla \mathcal{M}_i(\mathbf{h}_i^{(k)}) \right]^\top \nabla \mathcal{M}_i(\mathbf{h}_i^{(k)}) + \right. \\ & \left. \int_0^1 \left\| \eta \nabla \mathcal{M}_i(\mathbf{h}_i^{(k)}) \right\| \left\| 2\theta \eta \left(1 - \frac{\mathbf{A}(i, i)}{\mathbf{D}(i, i)} \right) \nabla \mathcal{M}_i(\mathbf{h}_i^{(k)}) \right\| d\theta \right\} \\ &\leq \sum_{i=1}^{|\mathcal{V}|} \left[\mathcal{M}_i(\mathbf{h}_i^{(k)}) - (\eta - \eta^2) \left\| \nabla \mathcal{M}_i(\mathbf{h}_i^{(k)}) \right\|^2 \right]. \end{aligned} \quad (12)$$

The Eq. (12) indicates that when $0 \leq \eta \leq 1$, the inequality $\sum_{i=1}^{|\mathcal{V}|} \mathcal{M}_i(\mathbf{h}_i^{(k)} - \eta \nabla \mathcal{M}_i(\mathbf{h}_i^{(k)})) \leq \sum_{i=1}^{|\mathcal{V}|} \mathcal{M}_i(\mathbf{h}_i^{(k)})$ always holds. We have shown in Eq. (11) that $\mathbf{h}_i^{(k+1)} = \mathbf{h}_i^{(k)} - \frac{1}{2} \nabla \mathcal{M}_i(\mathbf{h}_i^{(k)})$, so Eq. (12) at $\eta = \frac{1}{2}$ can be written as:

$$\begin{aligned} \sum_{i=1}^{|\mathcal{V}|} \mathcal{M}_i(\mathbf{h}_i^{(k+1)}) &= \sum_{i=1}^{|\mathcal{V}|} \mathcal{M}_i\left(\mathbf{h}_i^{(k)} - \frac{1}{2} \nabla \mathcal{M}_i(\mathbf{h}_i^{(k)})\right) \\ &\leq \sum_{i=1}^{|\mathcal{V}|} \mathcal{M}_i(\mathbf{h}_i^{(k)}). \end{aligned} \quad (13)$$

This implies that the variation of node embeddings decreases (shrinking) as the message passing proceeds. In other words, embeddings of nodes shrink into distinct clusters in the space based on the graph topology. The motivation of the proposed methods is to eliminate unreliable connections in the graph topology, allowing related nodes (e.g., nodes of the same class) to be connected as much as

possible. This enables the embeddings to shrink into distinct clusters according to their classes, thus clarifying the classification boundaries and enhancing the model’s performance.

4 EXPERIMENTS

4.1 Experimental Setting

Datasets and baselines. Experiments are conducted on four real-world TAGs: Cora [21], Citeseer [7], Pubmed [29], Arxiv-2023 [10]. The statistics of these datasets are detailed in Table 1. We evaluate our approach by comparing it against the following baselines. (1) GCN [17]: GCN is regarded as a pioneering work in GNNs, which obtains high-quality node embeddings by aggregating feature information from the neighbors of each node. (2) GAT [32]: GAT leverages the attention mechanism to assign different weights to nodes within a neighborhood. Essentially, the GAT can also be viewed as a method aimed at optimizing graph topology. (3) GCN-LPA [34]: GCN-LPA combines the GCN with LPA, where the LPA acts as regularization to guide the GCN in learning proper edge weights. (4) LLM: We use the gpt-3.5-turbo [1] to identify the categories of nodes in the TAG. Specifically, we take the text attributes of nodes (i.e. paper title and abstract) as input and obtain category information from the output of the gpt-3.5-turbo. (5) TAPE [10]: TAPE is the SOTA paradigm combining LLMs and GNNs.

4.2 Implementation Details

We adopt the GCN as the underlying graph learning architecture to validate the effect of LLM-based topology perturbations. The hyperparameters used for the GCN are consistent with previous studies [10, 12]. As our goal is to investigate the effects of topology modifications, the hyperparameters associated with the GCN structure are not tuned specifically for each dataset. Considering the expenses associated with querying LLMs’ APIs and the rate limit imposed by OpenAI, we randomly select 1,000 edges as candidate edges for edge deletion/addition in each dataset. For edge deletion, we choose candidate edges from the existing edges in each dataset. For edge addition, we select candidate edges based on the second-order neighbors of the nodes. Specifically, if two nodes are second-order neighbors and there is no existing edge between them, these two nodes will be considered as candidate node pairs for edge addition. The threshold ξ used in the deletion/addition process is tuned between 0.1 and 0.9 with an interval of 0.1. The hyperparameters λ and β used in the LLM-based pseudo-label propagation are tuned between 0 and 5 (interval 0.1). For the general setting, 60% of the nodes are designated for the training set, 20% for the validation set, and the remaining 20% are set aside for the test set. For the few-shot setting, we randomly select 20 nodes from each class to

form the training set, 500 random nodes for the validation set, and 1,000 random nodes from the remaining pool for the test set.

4.3 Performance Comparisons

General setting. Table 2 shows the experimental results under the general setting, where “LLM-based A-D” represents “LLM-based Edge Deletion and Edge Addition”, “LLM-based LPA” represents “LLM-based Pseudo-label Propagation”, and “LLM-based A-D & LPA” represents the combination of “LLM-based A-D” and “LLM-based LPA”. It can be seen that the LLM-based topological structure perturbation has certain positive effects. The “GCN + LLM-based A-D” can achieve performance gains compared to the GCN in most cases. This is attributed to the powerful text understanding ability of the LLM, which enables it to filter out unreliable edges in the graph and add reliable ones (please refer to the Sec. 4.5 Case Study for more details), thereby enhancing the quality of the learned representations (through facilitating the process of message passing). Similar performance gains can be observed in the “GCN + LLM-based LPA”. Compared to the classical label propagation method like GCN-LPA, the LLM-based pseudo-label propagation introduces more label information by utilizing the powerful reasoning capabilities of the LLM. Specifically, the GCN-LPA only uses the labels of labeled nodes (unlabeled nodes use a default label) during label propagation, whereas the “GCN + LLM-based LPA” not only uses the labels of labeled nodes, but also high-quality pseudo-labels generated by the LLM for unlabeled nodes. The additional label information aids label propagation, which in turn helps guide the model to learn more proper edge weights (i.e., a better graph topology). Although the LLM-based edge deletion/addition and the LLM-based pseudo-label propagation have differences in the direction of optimizing the graph topology, we find that combining the two can further enhance the model performance. As shown in the Table 2, the “GCN + LLM-based A-D & LPA” is almost always the top performer across all settings under the traditional paradigm. We also verify the generalizability of the refined graph topology structure on the SOTA paradigm TAPE, i.e., using the “TA+P+E” feature [10]. “TA+P+E” feature is a recently proposed LLM-augmented feature that incorporates the original features of the TAG (TA), LLM explanations (E), and LLM predictions (P). The results demonstrate that the LLM-based graph topology refinement approaches also benefit learning with the “TA+P+E” feature, showcasing the versatility of the proposed methods to some extent.

Few-shot setting. To further demonstrate the impact of pseudo-labels generated by the LLM on the label propagation, we test the performance of the “GCN + LLM-based LPA” in the few-shot setting, as shown in the Table 3. The “GCN + LLM-based LPA” has achieved performance gains in different scenarios, which is consistent with the experimental results under the general setting. We also test the generalizability of the optimized graph topology structure on the SOTA paradigm TAPE. The experimental results demonstrate that the LLM-based graph topology perturbation also improves learning with the “TA+P+E” feature under the few-shot setting.

4.4 Visualization and Analysis

In Fig. 4, we present heatmaps and contour plots on different datasets, which are obtained by adjusting the thresholds used in

Table 1: Statistics of TAGs.

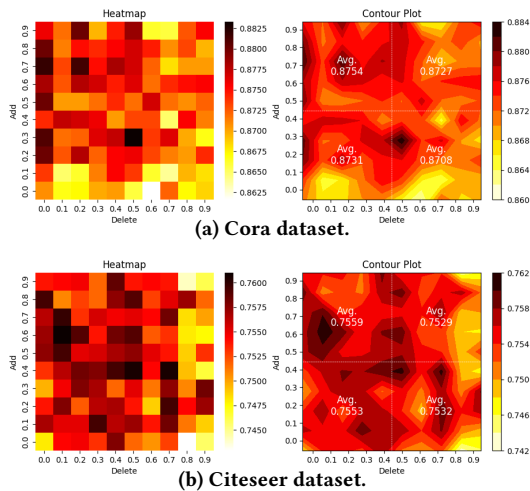
Dataset	#Nodes	#Edges	Task	Metric
Cora	2,708	5,429	7-class node classification	Accuracy
Citeseer	3,186	4,277	6-class node classification	Accuracy
Pubmed	19,717	44,338	3-class node classification	Accuracy
Arxiv-2023	46,198	78,548	40-class node classification	Accuracy

Table 2: Results of the proposed methods on four public datasets in the general setting (Best, second Best).

Dataset	Cora	Pubmed	Citeseer	Arxiv-2023
LLM	0.6769 ± 0.0000	0.9342 ± 0.0000	0.5929 ± 0.0000	0.7356 ± 0.0000
GAT	0.8750 ± 0.0084	0.9312 ± 0.0083	0.7547 ± 0.0231	0.7704 ± 0.0043
GCN	0.8778 ± 0.0137	0.9314 ± 0.0039	0.7508 ± 0.0066	0.7694 ± 0.0022
GCN-LPA	0.8750 ± 0.0209	0.9446 ± 0.0030	0.7559 ± 0.0104	0.7831 ± 0.0038
GCN + llm-based A-D	<u>0.8815 ± 0.0180</u>	0.9309 ± 0.0050	0.7578 ± 0.0079	0.7708 ± 0.0009
GCN + llm-based LPA	0.8828 ± 0.0191	<u>0.9469 ± 0.0037</u>	<u>0.7614 ± 0.0149</u>	<u>0.7853 ± 0.0022</u>
GCN + llm-based A-D & LPA	0.8778 ± 0.0183	0.9475 ± 0.0036	0.7633 ± 0.0117	0.7858 ± 0.0027
TAPE _{GAT}	0.8838 ± 0.0088	0.9316 ± 0.0115	0.7610 ± 0.0107	0.7807 ± 0.0023
TAPE _{GCN}	0.8833 ± 0.0046	0.9319 ± 0.0037	0.7571 ± 0.0046	0.7819 ± 0.0027
TAPE _{GCN-LPA}	0.8824 ± 0.0051	0.9461 ± 0.0023	0.7653 ± 0.0073	0.8020 ± 0.0029
TAPE _{GCN} + llm-based A-D	<u>0.8907 ± 0.0138</u>	0.9329 ± 0.0045	0.7625 ± 0.0101	0.7840 ± 0.0012
TAPE _{GCN} + llm-based LPA	0.8875 ± 0.0151	0.9475 ± 0.0049	0.7692 ± 0.0059	0.8033 ± 0.0037
TAPE _{GCN} + llm-based A-D & LPA	0.8916 ± 0.0096	<u>0.9472 ± 0.0056</u>	<u>0.7684 ± 0.0076</u>	<u>0.8032 ± 0.0023</u>

Table 3: Results of the proposed methods on four public datasets in the few-shot setting (Best, second Best).

Dataset	Cora	Pubmed	Citeseer	Arxiv-2023
GAT	0.7272 ± 0.0315	0.6462 ± 0.0685	<u>0.6703 ± 0.0429</u>	0.4185 ± 0.1070
GCN	0.7552 ± 0.0094	<u>0.6462 ± 0.0664</u>	0.6647 ± 0.0337	0.4960 ± 0.0458
GCN-LPA	<u>0.7588 ± 0.0132</u>	0.6382 ± 0.0550	0.6657 ± 0.0319	<u>0.5050 ± 0.0437</u>
GCN + llm-based LPA	0.7630 ± 0.0134	0.6535 ± 0.0427	0.6780 ± 0.0341	0.5175 ± 0.0392
TAPE _{GAT}	0.7990 ± 0.0054	0.8573 ± 0.0107	<u>0.7223 ± 0.0240</u>	0.6747 ± 0.0826
TAPE _{GCN}	0.8190 ± 0.0050	0.8668 ± 0.0147	0.7200 ± 0.0168	0.7365 ± 0.0271
TAPE _{GCN-LPA}	<u>0.8232 ± 0.0033</u>	<u>0.8815 ± 0.0195</u>	0.7198 ± 0.0084	<u>0.7382 ± 0.0278</u>
TAPE _{GCN} + llm-based LPA	0.8275 ± 0.0066	0.8930 ± 0.0256	0.7307 ± 0.0143	0.7428 ± 0.0272

**Figure 4: Heatmaps and contour plots on different datasets.**

the edge deletion and addition processes. From these heatmaps and contour plots, we can observe a consistent pattern: the values in the top left corner of the figures are relatively large, while the values in the bottom right corner are relatively small. In other words, adding edges that LLM considers reliable and deleting those are considered as unreliable is beneficial to improving the topological structure,

thereby improving the classification accuracy. For example, in the contour plot of the Cora dataset, the average accuracy in the top left corner is 0.8754, while in the bottom right corner it is 0.8708. This phenomenon indicates that LLMs do have the ability to make reasonable edge additions and deletions based on the semantics of the input text.

4.5 Case study

Different prompt statements. In this part, we analyze the impact of different prompt statements. The details of the six different prompts are shown as follows:

Prompt 1: Do not give any examples

Your task is to calculate the similarity between the given two papers.

Paper A:

Title: [paper title ...] Abstract: [paper abstract ...]

Paper B:

Title: [paper title ...] Abstract: [paper abstract ...]

Your return form is: Related ratio = ***, Reason: ***.

Prompt 2: Give only a few examples (one example)

Your task is to calculate the similarity between the given two

papers. Here is an example, where the input is the information for paper A and paper B, and the output is the estimated related ratio between paper A and paper B:

Example 1:

...

Please return the similarity between the following two papers and briefly explain the reason:

Paper A:

Title: [paper title ...] Abstract: [paper abstract ...]

Paper B:

Title: [paper title ...] Abstract: [paper abstract ...]

Your return form is: Related ratio = ***, Reason: ***.

Prompt 3: Give only a few examples (two examples)

Your task is to calculate the similarity between the given two papers. Here is an example, where the input is the information for paper A and paper B, and the output is the estimated related ratio between paper A and paper B:

Example 1-2:

...

Please return the similarity between the following two papers and briefly explain the reason:

Paper A:

Title: [paper title ...] Abstract: [paper abstract ...]

Paper B:

Title: [paper title ...] Abstract: [paper abstract ...]

Your return form is: Related ratio = ***, Reason: ***.

Prompt 4: Ask directly if there is a link between nodes

Do you think there should be a link (or edge) between paper A and paper B below?

Paper A:

Title: [paper title ...] Abstract: [paper abstract ...]

Paper B:

Title: [paper title ...] Abstract: [paper abstract ...]

If you think there is a link (or edge) between the two papers above, please return YES, otherwise please return NO. You need to briefly explain why.

Prompt 5: Do not ask for a reason/explanation for the LLM's response

Your task is to calculate the similarity between the given two papers. Here are some examples, where the input is the information for paper A and paper B, and the output is the estimated related ratio between paper A and paper B:

Examples 1–4:

...

Please only return the similarity between the following two papers:

Paper A:

Title: [paper title ...] Abstract: [paper abstract ...]

Paper B:

Title: [paper title ...] Abstract: [paper abstract ...]

Your return form is: Related ratio = ***.

Prompt 6: The prompt used in this paper

Your task is to calculate the similarity between the given two papers. Here are some examples, where the input is the information for paper A and paper B, and the output is the estimated related ratio between paper A and paper B:

Example 1–4:

...

Please return the similarity between the following two papers and briefly explain the reason:

Paper A:

Title: [paper title ...] Abstract: [paper abstract ...]

Paper B:

Title: [paper title ...] Abstract: [paper abstract ...]

Your return form is: Related ratio = ***, Reason: ***.

In prompt 1, we do not provide any examples to the LLM. Prompt 2 and prompt 3, on the other hand, included a few examples given to the LLM as references. Instead of asking for similarity, we directly ask the LLM to determine whether there is an edge between nodes in prompt 4. In prompt 5, we do not require the LLM to provide an explanation for its response. Prompt 6, which is used in this paper, includes 4 examples and requests the LLM to assess the semantic similarity/relevance between pairs of text and provide an explanation. The experimental results are shown in Table 4. As shown in Table 4, increasing the number of examples helps the LLM make more reasonable judgments. For example, the performance of the model using prompt 6 (with 4 examples) is better than the performance of the model using prompt 1 (without examples). Directly asking the LLM whether links or edges exist between nodes does not yield good results. This may be because the concept of links/edges is too abstract and cannot be well understood by the LLM. The prompt statement that requesting explanations from the LLM does not significantly improve the model performance. Nevertheless, the explanations provided by the LLM are beneficial for understanding the underlying logic behind its responses, which in turn facilitates qualitative analysis of the potential of the LLM in topology enhancement.

Table 4: Applying different prompt statements on the Cora dataset.

Prompt	TA	TA+P+E
Prompt 1	0.8768 ± 0.0093	0.8768 ± 0.0238
Prompt 2	0.8792 ± 0.0196	0.8884 ± 0.0111
Prompt 3	0.8801 ± 0.0168	0.8787 ± 0.0152
Prompt 4	0.8718 ± 0.0232	0.8782 ± 0.0115
Prompt 5	0.8815 ± 0.0178	0.8838 ± 0.0121
Prompt 6	0.8815 ± 0.0180	0.8907 ± 0.0138

Examples of user queries and LLM responses. In this part, we employ specific examples for qualitative analysis. There are two examples provided: one of them are related to the LLM-based edge deletion/addition and one is about the generation of pseudo-labels for the LLM-based pseudo-label propagation. The first example is shown below:

User query

Your task is to calculate the similarity between the given two papers. Here are some examples ...

Examples 1-4:
[Input]... [Output]...
...

Please return the similarity between the following two papers and briefly explain the reason:

Paper A:
Title: Supervised learning from incomplete data via an EM approach. Abstract: Real-world learning tasks may involve high-dimensional data sets with arbitrary patterns of missing data. In this paper, we present a framework based on maximum likelihood density estimation for learning from such data sets ...

Paper B:
Title: Using Temporal-Difference Reinforcement Learning to Improve Decision-Theoretic Utilities for Diagnosis. Abstract: Probability theory represents and manipulates uncertainties, but cannot tell us how to behave. For that we need utility theory which assigns values to the usefulness of different states, ...

Your return form is: Related ratio = **, Reason: **.

LLM response

Related ratio = 0.1. **Reason:** There is minimal similarity between Paper A and Paper B. Paper A discusses supervised learning from incomplete data using an EM approach, while Paper B focuses on using temporal-difference reinforcement learning to improve decision-theoretic utilities for diagnosis. The topics and methodologies discussed in the two papers are quite different, resulting in a low related ratio.

In this case, one node corresponds to a paper discussing a framework based on maximum likelihood density estimation for learning from datasets with arbitrary patterns of missing data, while the other node corresponds to a paper discussing the application of reinforcement learning in diagnostic scenarios. The contents of these two papers have almost no overlap, therefore the LLM considers it reasonable that the related ratio between the two nodes is low (i.e., 0.1). Additionally, the explanation provided by the LLM for why it gave such a response is in line with human understanding. In its explanation, the LLM emphasizes the significant differences in both the topic and methodology of the papers corresponding to these two nodes, which is consistent with our previous analysis.

In the second case, we provide an example about the generation of pseudo-labels, as follows:

User query

The title and abstract of the paper are as follows: A Case for Parallelism in Data Warehousing and OLAP. In recent years the database community has experienced a tremendous increase in the availability of new technologies to support efficient storage and retrieval of large volumes of data ...

Question: Which of the following subcategories does this paper belong to: (A) Agents, (B) Artificial Intelligence, (C) Database, (D) Human Computer Interaction, (E) Machine Learning, (F) Information Retrieval? If multiple options apply, provide a comma-separated list ordered from most to least related, then for each choice you gave, explain how it is present in the text.

Answer:

LLM response

The subcategory that this paper belongs to is (C) Database. In the text, the paper discusses the database community's increased availability of new technologies for efficient storage and retrieval of large volumes of data. It specifically focuses on data warehousing and On-Line Analytical Processing (OLAP) products, which are database technologies. The paper proposes a solution approach to improve query processing times in a data warehouse environment, which is directly related to database management. Additionally, the paper discusses efficient partitioning, indexing strategy, and parallel resource utilization, all of which are important concepts in database systems.

This case presents a database-related paper that investigates query processing efficiency in data warehousing and OLAP. It proposes applying parallel processing techniques to reduce response time. The LLM accurately gives the subcategory to which this paper belongs and gives a detailed explanation. In the explanation of LLM, it is not difficult to observe that the LLM pays attention to several key database-related technologies in the paper, such as data warehousing, efficient partitioning, and indexing strategy. These database-related technologies lead the LLM to infer that this paper belongs to the database category. It can be seen that the logic behind LLM's explanation closely aligns with human reasoning. The impressive text comprehension ability of LLM serves as a guarantee for generating high-quality pseudo-labels, which paves the way for the proposed LLM-based pseudo-label propagation.

5 RELATED WORK

Label Propagation. Traditional LPAs solely rely on labels and do not consider features [37]. To better utilize the information contained in node features, various techniques have been proposed for learning edge weights (i.e., adaptive LPAs), including using kernel functions [20, 39], minimizing neighborhood reconstruction error [16, 33], and imposing sparsity constraints [11]. Wang et al. proposed an approach using LPA itself as a regularization to help the model learn edge weights [34], which is different from the adaptive LPA that mentioned above using a specific regularization (e.g., reconstruction error). However, the initial label matrix used for label propagation in [34] is constructed solely using the information from labeled nodes, while ignoring the information in unlabeled nodes. In this paper, we utilize LLMs to generate high-quality pseudo labels to assist label propagation, which enables the

information in unlabeled nodes to be utilized to some extent as well, thereby guiding the model to learn more proper edge weights.

Applying LLMs on TAGs. LLMs [1, 5, 31] have demonstrated great potential in various NLP tasks. However, how to apply LLMs to graph-structured data, such as TAGs, remains a challenge [2, 26, 30, 36]. Chen et al. investigate the potential of LLMs in node classification tasks [4]. He et al. propose a novel feature ‘TAPE’ augmented by the LLM [10], which incorporates the original attributes of nodes in the TAG, predictions made by the LLM on node categories, as well as explanations from the LLM for making such predictions. As shown before, existing methods primarily utilize LLMs to enhance the node features in graphs. However, approaches leveraging LLMs to aid the enhancement of graph topological structures remain relatively underexplored. In this paper, we focus on exploring LLMs’ potential in enhancing graph topological structures.

6 CONCLUSION

In this paper, we investigate the potential of LLMs in refining graph topology. First, we explore the way to leverage LLMs’ capabilities in deleting the unreliable edges and adding reliable edges in the TAG through the prompt statement. Second, considering LLMs’ text understanding and information retrieval abilities can help generate high-quality pseudo-labels, we propose to leverage the pseudo-labels produced by LLMs to improve the topological structure of TAGs (through the label propagation). Finally, we integrate the above two topological refinement methods into the process of GNN training. The experimental results demonstrate that LLMs can play a positive role in perturbing the topological structure of graphs.

REFERENCES

- Tom Brown et al. 2020. Language Models are Few-Shot Learners. In *Advances in Neural Information Processing Systems*.
- Ziwei Chai, Tianjie Zhang, Liang Wu, Kaiqiao Han, Xiaohai Hu, Xuanwen Huang, and Yang Yang. 2023. GraphLLM: Boosting Graph Reasoning Ability of Large Language Model. In *arXiv:2310.05845*.
- Yupeng Chang, Xu Wang, Jindong Wang, Yuan Wu, Linyi Yang, Kaijie Zhu, Hao Chen, Xiaoyuan Yi, Cunxiang Wang, Yidong Wang, Wei Ye, Yue Zhang, Yi Chang, Philip S. Yu, Qiang Yang, and Xing Xie. 2023. A Survey on Evaluation of Large Language Models. In *arXiv:2307.03109*.
- Zhikai Chen, Haitao Mao, Hang Li, Wei Jin, Hongzhi Wen, Xiaochi Wei, Shuaiqiang Wang, Dawei Yin, Wenqi Fan, Hui Liu, and Jiliang Tang. 2023. Exploring the Potential of Large Language Models (LLMs) in Learning on Graphs. In *arXiv:2307.03393*.
- Aakanksha Chowdhery et al. 2022. PaLM: Scaling Language Modeling with Pathways. In *arXiv:2204.02311*.
- Jacob Devlin, Ming-Wei Chang, Kenton Lee, and Kristina Toutanova. 2023. BERT: Pre-training of Deep Bidirectional Transformers for Language Understanding. In *NAACL*.
- Clyde Lee Giles, Kurt Dewitt Bollacker, and Steve Lawrence. 1998. CiteSeer: An Automatic Citation Indexing System. In *Proc. ACM Conf. Digital Libraries*.
- William L. Hamilton, Zhitao Ying, and Jure Leskovec. 2017. Inductive Representation Learning on Large Graphs. In *Advances in Neural Information Processing Systems*.
- Pengcheng He, Xiaodong Liu, Jianfeng Gao, and Weizhu Chen. 2020. DeBERTa: Decoding-enhanced Bert with Disentangled Attention. In *arXiv:2006.03654*.
- Xiaoxin He, Xavier Bresson, Thomas Laurent, Adam Perold, Yann LeCun, and Bryan Hooi. 2023. Harnessing Explanations: LLM-to-LM Interpreter for Enhanced Text-Attributed Graph Representation Learning. In *arXiv:2305.19523*.
- Cheng Hong, Zicheng Liu, and Jie Yang. 2009. Sparsity Induced Similarity Measure for Label Propagation. In *Proc. IEEE Int. Conf. Computer Vision*.
- Weihua Hu, Matthias Fey, Marinka Zitnik, Yuxiao Dong, Hongyu Ren, Bowen Liu, Michele Catasta, and Jure Leskovec. 2020. Open Graph Benchmark: Datasets for Machine Learning on Graphs. *arXiv:2005.00687* (2020).
- Dejun Jiang, Zhenxing Wu, Chang-Yu Hsieh, Guangyong Chen, Ben Liao, Zhe Wang, Chao Shen, Dongsheng Cao, Jian Wu, and Tingjun Hou. 2021. Could Graph Neural Networks Learn Better Molecular Representation for Drug Discovery? A Comparison Study of Descriptor-based and Graph-based Models. *Journal of Cheminformatics* (2021).
- Armand Joulin, Edouard Grave, Piotr Bojanowski, Matthijs Douze, Herve Jégou, and Tomas Mikolov. 2016. FastText.zip: Compressing Text Classification Models. In *arXiv:1612.03651*.
- Jared Kaplan, Sam McCandlish, Tom Henighan, Tom Brown, Benjamin Chess, Rewon Child, Scott Gray, Alec Radford, Jeffrey Wu, and Dario Amodei. 2020. Scaling Laws for Neural Language Models. In *arXiv:2001.08361*.
- Masayuki Karasuyama and Hiroshi Karasuyama. 2013. Manifold-based Similarity Adaptation for Label Propagation. In *Advances in Neural Information Processing Systems*.
- Thomas N. Kipf and Max Welling. 2016. Semi-Supervised Classification with Graph Convolutional Networks. In *Proc. Int. Conf. Learning Representations*.
- Shuangli Li, Jingbo Zhou, Tong Xu, Liang Huang, Fan Wang, Haoyi Xiong, Weili Huang, Dejiong Dou, and Hui Xiong. 2021. Structure-aware Interactive Graph Neural Networks for the Prediction of Protein-Ligand Binding Affinity. In *Proc. ACM Conf. Knowledge Discovery and Data Mining*.
- Xiao Lin, Jian Kang, Weilin Cong, and Hanghang Tong. 2023. BeMap: Balanced Message Passing for Fair Graph Neural Network. In *LoG*.
- Yanbin Liu, Juho Lee, Minseop Park, Saehoon Kim, Eunho Yang, Sung Ju Hwang, and Yi Yang. 2019. Learning to Propagate Labels: Transductive Propagation Network for Few-shot Learning. In *Proc. Int. Conf. Learning Representations*.
- Andrew Kachites McCallum, Kamal Nigam, Jason Rennie, and Kristie Seymore. 2000. Automating the Construction of Internet Portals with Machine Learning. *Information Retrieval* 3 (2000), 127–163.
- Alessio Miaschi and Felice Dell’Orletta. 2020. Contextual and Non-Contextual Word Embeddings: an in-depth Linguistic Investigation. In *ACL*.
- Tomas Mikolov, Kai Chen, Greg Corrado, and Jeffrey Dean. 2013. Efficient Estimation of Word Representations in Vector Space. In *arXiv:1301.3781*.
- Seth A. Myers, Aneesh Sharma, Pankaj Gupta, and Jimmy Lin. 2014. Information Network or Social Network? The Structure of the Twitter Follow Graph. In *Proc. Int. Conf. World Wide Web*.
- OpenAI. 2023. Gpt-4 Technical Report. In *arXiv:2303.08774*.
- Yijian Qin, Xin Wang, Ziwei Zhang, and Wenwu Zhu. 2023. Disentangled Representation Learning with Large Language Models for Text-Attributed Graphs. In *arXiv:2310.18152*.
- XiPeng Qiu, TianXiang Sun, YiGe Xu, YunFan Shao, Ning Dai, and XuanJing Huang. 2020. Pre-trained Models for Natural Language Processing: A Survey. *Science China Technological Sciences* 63, 10 (2020), 1872–1897.
- Michael Schlichtkrull, Thomas N. Kipf, Peter Bloem, Rianne van den Berg, Ivan Titov, and Max Welling. 2017. Modeling Relational Data with Graph Convolutional Networks. In *arXiv:1703.06103*.
- Prithviraj Sen, Galileo Namata, Mustafa Bilgic, Lise Getoor, Brian Galligher, and Tina Eliassi-Rad. 2008. Collective Classification in Network Data. *AI Magazine* 29, 3 (2008), 93–106.
- Jiabao Tang, Yuhao Yang, Wei Wei, Lei Shi, Lixin Su, Suqi Cheng, Dawei Yin, and Chao Huang. 2023. GraphGPT: Graph Instruction Tuning for Large Language Models. In *arXiv:2310.13023*.
- Hugo Touvron, Thibaut Lavril, Gautier Izacard, Xavier Martinet, Marie-Anne Lachaux, Timothée Lacroix, Baptiste Rozière, Naman Goyal, Eric Hambro, Faisal Azhar, Aurelien Rodriguez, Armand Joulin, Edouard Grave, and Guillaume Lample. 2023. LLaMA: Open and Efficient Foundation Language Models. In *arXiv:2302.13971*.
- Petar Velickovic, Guillem Cucurull, Arantxa Casanova, Adriana Romero, Pietro Liò, and Yoshua Bengio. 2018. Graph Attention Networks. In *Proc. Int. Conf. Learning Representations*.
- Fei Wang and Changshui Zhang. 2008. Label Propagation through Linear Neighborhoods. *IEEE Trans. Knowledge and Data Engineering* (2008).
- Hongwei Wang and Jure Leskovec. 2021. Combining Graph Convolutional Neural Networks and Label Propagation. *ACM Trans. Information Systems* 40, 4 (2021), 1–27.
- Menglin Yang, Ziqiao Meng, and Irwin King. 2020. L2 Feature Normalization for Dynamic Graph Embedding. In *Proc. IEEE Int. Conf. Data Mining*.
- Haiteng Zhao, Shengchao Liu, Chang Ma, Hannan Xu, Jie Fu, Zhi-Hong Deng, Lingpeng Kong, and Qi Liu. 2023. GIMLET: A Unified Graph-Text Model for Instruction-Based Molecule Zero-Shot Learning. In *arXiv:2306.13089*.
- Dengyong Zhou, Olivier Bousquet, Thomas Navin Lal, Jason Weston, and Bernhard Schölkopf. 2004. Learning with Local and Global Consistency. In *Advances in Neural Information Processing Systems*.
- Denny Zhou and Bernhard Schölkopf. 2005. Regularization on Discrete Spaces. In *DAGM Symposium*.
- Xiaojin Zhu, Zoubin Ghahramani, and John Lafferty. 2003. Semi-supervised Learning Using Gaussian Fields and Harmonic Functions. In *Proc. Int. Conf. Machine Learning*.